Dual-wavelength waveguide lasers at 1064 and 1079 nm in Nd:YAP crystal by direct femtosecond laser writing

Article *in* Optics Letters · May 2015

DOI: 10.1364/OL.40.002437

6 authors, including:

Weijie Nie
Shandong University
21 PUBLICATIONS **220** CITATIONS

Chen Cheng
Shandong University
36 PUBLICATIONS **537** CITATIONS

Yuechen Jia
Shandong University
71 PUBLICATIONS **822** CITATIONS

Carolina Romero
Universidad de Salamanca
68 PUBLICATIONS **498** CITATIONS

Dual-wavelength waveguide lasers at 1064 and 1079 nm in Nd:YAP crystal by direct femtosecond laser writing

Weijie Nie,[1] Chen Cheng,[1] Yuechen Jia,[1] Carolina Romero,[2] Javier R. Vázquez de Aldana,[2] and Feng Chen[1,]*

[1]*School of Physics, State Key Laboratory of Crystal Materials, Shandong University, Jinan 250100, China*

[2]*Laser Microprocessing Group, Universidad de Salamanca, Salamanca 37008, Spain*

**Corresponding author: drfchen@sdu.edu.cn*

Received March 25, 2015; revised April 28, 2015; accepted May 3, 2015;
posted May 5, 2015 (Doc. ID 236916); published May 15, 2015

Low-loss depressed cladding waveguides have been produced in Nd:YAP laser crystal by using direct femtosecond laser writing. Under optical pump at 812 nm at room temperature, continuous-wave simultaneous dual-wavelength laser oscillations at 1064 and 1079 nm, both along TM polarization, have been realized in the waveguiding structures. It has been found that, with the variation of pump polarization, the intensity ratio of 1064 and 1079 nm emissions varies periodically, while the polarization of output dual-wavelength laser remains unchanged. The maximum output power achieved for the Nd:YAP waveguide lasers is ~200 mW with a slope efficiency of 33.4%.

OCIS codes: (230.7370) Waveguides; (140.3390) Laser materials processing; (130.3120) Integrated optics devices.
http://dx.doi.org/10.1364/OL.40.002437

Dual-wavelength lasing from a single laser medium [1,2] has attracted great interest due to many different potential applications in high-precision laser metrology, laser spectroscopy, laser probing, analysis of the atmosphere, laser medium treatment or THz research, and other areas. In order to generate the dual-wavelength lasers, Nd-doped crystals are excellent candidates as the gain medium owing to the multiple energy levels of incorporated active ions [3,4]. The neodymium-doped yttrium aluminate (Nd:$YAlO_3$ or Nd:YAP) crystal is one of the well-known candidates for dual-wavelength lasing due to its high thermal conductivity, excellent optomechanical coefficient, and large stimulated emission cross-sections [5]. The most frequently used laser line corresponds to the $^4F_{3/2} \rightarrow {}^4I_{11/2}$ transition, which has two intense overlapped stark transitions of R1–Y1 at 1064 nm and R2–Y3 at 1079 nm [6]. For the transmission along the c-axis of the crystal, the laser gain at 1079 nm (1064 nm) is the largest when the pump light is polarized along a-axis (b-axis). However, the emission cross-section at 1079 nm ($\sigma = 24 \times 10^{-19}$ cm^2) is almost identical to that at 1064 nm ($\sigma = 25 \times 10^{-19}$ cm^2); as a result, the competition between the two wavelengths will occur according to the polarization of the pump light. In addition, owing to its biaxiality, the gain coefficient and polarization of stimulated emission cross-section can be varied with the crystallographic orientation of the laser crystal, which offers the possibility to optimize particular performance characteristics [7]. Moreover, the large natural birefringence of Nd:YAP may overcome the limitations on fundamental mode operation and depolarization losses caused by thermally induced stress birefringence and bifocusing at high average powers [8].

Optical waveguides, which are the basic elements for integrated photonic applications [9], can confine light in small volumes, reaching relatively high optical intensities inside the structure with respect to the bulks [10]. Benefiting from the compact geometry and the high intra-cavity intensity, waveguide lasers may possess superior performance compared to the bulk lasers [11]. For example, they have reduced lasing thresholds and enhanced slope efficiencies [12–14]. Waveguides in crystals could be fabricated by various approaches. The femtosecond laser inscription is a well-known technique to fabricate waveguides in transparent optical materials since 1996 [15–20], which has been widely utilized for three-dimensional (3D) materials microprocessing [21–23]. The femtosecond laser beam is focused at a sample spot producing a localized micro-modification of the materials with a refractive index change (negative or positive) [24] that can be used for waveguide fabrication. Depressed cladding waveguides (so-called Type III structures based on waveguide geometries) were first proposed by Okhrimchuk *et al.* [25]. They consist of an undamaged core surrounded by multiple low-index fs-laser inscribed tracks, and show many interesting features. For instance, the cross-section can be designed in circle geometry (or any arbitrary shape) with the required diameter, which may result in the high coupling efficiency between pump beams and guided modes [26]. In addition, the most unique ability of the cladding waveguides is that they can support efficient 2D guidance of light at two orthogonal polarizations, i.e., TE and TM polarizations, which is very promising for polarization-dependent guided-wave frequency conversion devices [24].

In this work, we report on the fabrication of Nd:YAP depressed-cladding waveguides by direct femtosecond laser writing. The continuous-wave (cw) dual-wavelength waveguide lasers at 1064 and 1079 nm with ratio tunable features based on $^4F_{3/2} \rightarrow {}^4I_{11/2}$ transitions have been realized under optical pump at 812 nm. The obtained waveguide lasers are with the fundamental-mode order, and always along vertical polarization (i.e., independent on the pump polarization).

The optically polished Nd:YAP crystal wafer was cut with the dimension of $2\ \mathrm{mm} \times 8\ \mathrm{mm} \times 10\ \mathrm{mm}$ ($b \times c \times a$). The depressed cladding waveguides (with a cross-sectional diameter of 100 μm) were produced by the laser facility of the Universidad de Salamanca, Spain. The structure consists of an unmodified core surrounded by a cladding of parallel low-index tracks,

0146-9592/15/102437-04$15.00/0

forming a circular shape. A Ti:sapphire amplifier (Spitfire, Spectra Physics) was used as laser source. It delivered linearly polarized pulses of 120 fs and 795-nm central wavelength, at 1-kHz repetition rate. The maximum available pulse energy was 1 mJ, and it was controlled by a calibrated neutral density filter placed after a set of half-wave plate and a linear polarizer. During the writing process of the cladding waveguide, the sample was located at a computer-controlled 3D-motorized stage. The laser beam was focused at 150 μm beneath one of the sample surfaces (with dimension of 8 mm × 10 mm) with a 40× microscope objective (N.A. = 0.65), and different pulse energies were tested, ranging from 0.1 to 1.5 μJ, finding an optimum value at 0.6 μJ that was used to fabricate the waveguides. While the sample was scanned at a constant velocity of 0.500 mm/s along the 8-mm edge, a damage line was produced inside the sample. The procedure was repeated at different positions of the sample, following the desired circular geometry with a lateral separation of 3 μm between each two adjacent damage tracks, resulting in the inscription of the depressed cladding waveguides.

The waveguide losses were evaluated by direct measurement of the input light power and output power of the transmitted light through a typical end-coupling system [27]. The obtained values for TM and TE modes at 1064 nm were 0.31 and 0.15 dB/cm, respectively. Compared with the reported value of an He^+ ion-implanted Nd:YAP planar waveguide (~15 dB/cm at ~610 nm) [28], the laser-written depressed cladding waveguide in this work shows superior guiding properties at the two orthogonal polarizations.

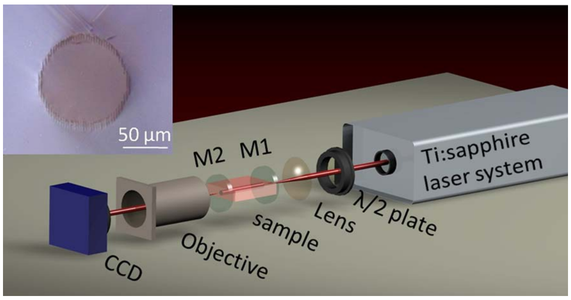

Fig. 1. Experimental setup for the dual-wavelength waveguide laser measurements. The inset shows the microscope cross-sectional image of the cladding waveguide with a diameter of 100 μm.

The dual-wavelength laser generation experiments were implemented with an end-face coupling system as shown in Fig. 1, and the inset of Fig. 1 shows the optical microscope cross-sectional image of the waveguide. A tunable cw Ti:sapphire laser (Coherent MBR PE), which was utilized as pump source, generated a linearly polarized beam at 812.3 nm. The polarization of the pump light was controlled by a half-wave plate, which was rotated from 0° to 180° so as to obtain thorough information of the polarization effects of the all-angle light transmission. The pump beam was converged to the input facet of sample by a spherical convex lens with a focal length of 75 mm and coupled into the waveguide. The laser oscillation cavity had a typical Fabry–Perot configuration constructed by two dielectric coupled mirrors that were adhered to the two polished end facets (a set of mechanical fixtures were used to press the two coupled mirrors for close contact with the two polished end facets of the waveguide sample). The input mirror (M_1) has a high transmission (98%) at 810 nm and high reflectivity (99%) at 1.06 μm, while the output mirror (M_2) has reflectivity of 99% at 810 nm and 90% at 1.06 μm. The generated lasers were collected with a 20× microscope objective lens (N.A. = 0.4) and were measured by a spectrometer, which was used to analyze the emission spectra and the relative intensity ratio.

As the polarization orientation of the pumping laser is changed, the lasing performance of the single- and dual-wavelength lasers varies alternately. Figure 2 depicts the spectra of laser emissions through the laser-writen Nd:YAP system. When the pumping laser is polarized at 0° (corresponding to the TE polarization of waveguide modes), the single-wavelength laser at 1079 nm is generated, as shown in Fig. 2(a). When the polarization is set to 45° (i.e., the ratio of TE to TM of pump light is 1∶1), the simultaneous dual-wavelength laser generation is obtained with an intensity ratio of ~1∶1 [see Fig. 2(b)]. When the pump light is with TM polarization, i.e., corresponding to 90° in Fig. 2(c), the single-wavelength laser operation at 1064 nm is achieved. It should be pointed out that, in all the cases, the waveguide lasers are with fundamental modes and nearly identical in profiles [see insets of Figs. 2(a)–2(c)]. In addition, the waveguide lasers at both 1064 and 1079 nm remained at the TM

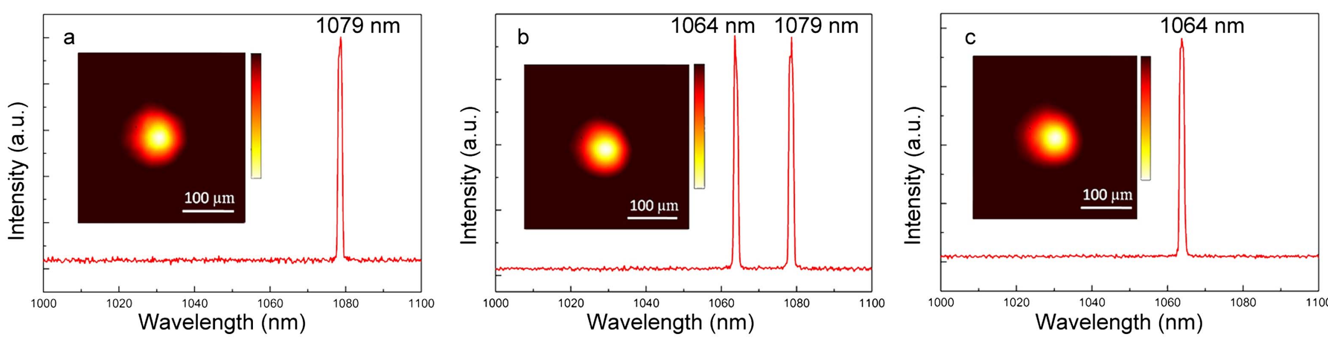

Fig. 2. The spectrum of laser emissions when the pumping laser polarized at (a) 0°, (b) 45°, and (c) 90°, respectively. The insets show the near-field profiles of TM_{00} modes.

direction, which is independent on the polarization pump light.

Figure 3(a) depicts the measured output laser power (i.e., the sum power of the 1064 and 1079 nm lasers) as a function of the launched pump power. From the linear fit of the experimental data, a lasing threshold of $P_{th} \approx 243.0$ mW and a slope efficiency of $\eta \approx 33.4\%$ are obtained for the laser-written Nd:YAP waveguide laser system. With the increase of the launched pump power, the output power of waveguide lasers rises to maximum $P_{max} \approx 199.8$ mW as the absorbed power reaches 831.6 mW. In order to investigate the effect of polarization of pump beam on the generated waveguide lasing, we have measured the output powers of lasing as a function of all-angle light pump with the same launched power at 812 nm [Fig. 3(b)]. As it can be seen in the figure, the total output power of 1064 and 1079 nm lasers is almost same for any polarization of pump light, i.e., nearly polarization-independent.

Although the sum power of dual-wavelength lasing remains same for pump of diverse polarizations, however, the output laser powers for separate 1064 and 1079 nm are polarization-dependent, as displayed in Fig. 4. Based on the nearly constant output power in Fig. 3(b), the relative laser intensity ratio of the two wavelengths in all-angle polarized plane is calculated. It has been found that the laser intensity ratio of 1064 and 1079 nm varies periodically with the variation of pump polarization. As the polarization rotated from 0° to 180°, the laser power

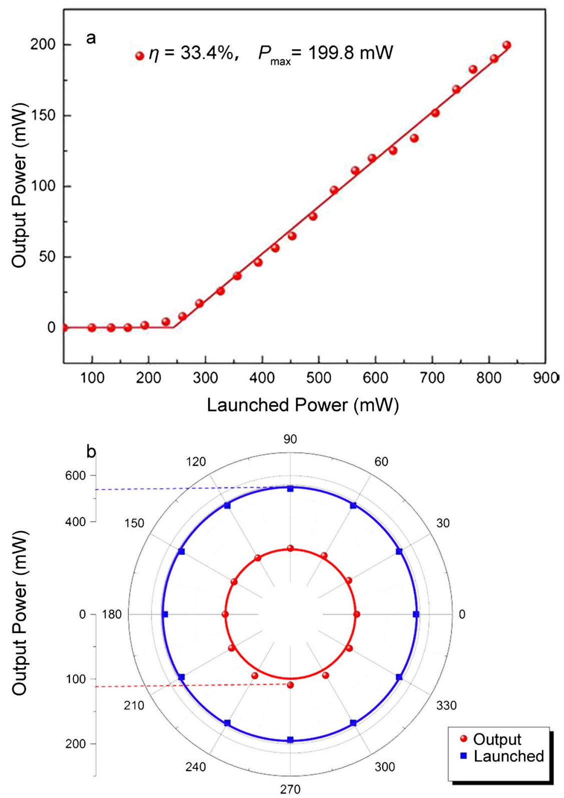

Fig. 3. (a) Output laser power as a function of the launched 812-nm pump power. The solid line represents the linear fit of the experimental data. (b) Output laser power as a function of all-angle light transmission with the same launched pump power at 812 nm.

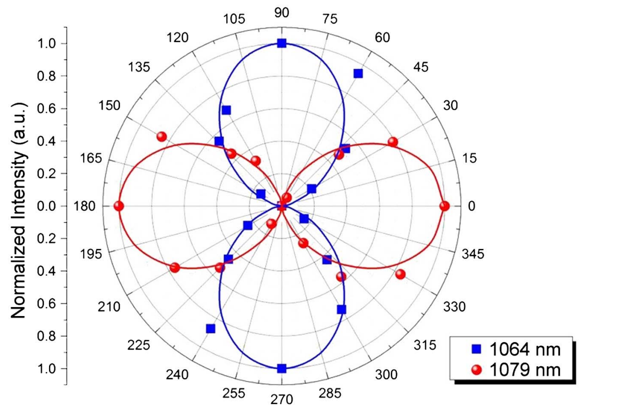

Fig. 4. Normalized laser intensity at 1064 (blue line) and 1079 nm (red line) as a function of the pump polarization.

at 1079 nm first decreases from its maximum to zero and then increases back, while the 1064-nm laser power shows the opposite behavior, being constantly the sum of both laser powers. When the pumping laser is polarized at 45° and 135°, the output laser powers at both wavelengths reach the same value. The variation curves shown in Fig. 4 are in good agreement with the results of Fig. 2, obtaining the laser performance from single- to dual-wavelength laser operation, as well as the wavelength switching from 1079 to 1064 nm. In addition, the intensity ratio of the 1064 and 1079 lasers is tunable, and, in principle, it could be any value between 0 and 1. This ratio-tunable feature of 1064- and 1079-nm waveguide lasers is first observed in the femtosecond laser-written systems.

In conclusion, we have fabricated the low-loss depressed cladding waveguide in Nd:YAP crystal by direct femtosecond laser writing. Efficient tunable dual-wavelength cw waveguide lasing is obtained at 1064 and 1079 nm, showing superior performance to the reported ion-implanted Nd:YAP planar waveguides [28]. The maximum output power of the waveguide laser was 199.8 mW with a slope efficiency of 33.4% under optical pump at 812 nm. It should be pointed out that the maximum output power of the cladding waveguide laser is limited by the power of the pumping laser in the system. The watt-level dual-wavelength waveguide laser could be expected in case of an efficient pump from fiber-coupled diode laser. In addition, the dual-wavelength waveguide laser operation in pulsed regimes could be realized in the Nd:YAP system by using appropriate saturable absorbers (e.g., graphene). And, an intriguing application of the Nd:YAP dual-wavelength waveguide laser system is to generate terahertz radiations with the small wavelength difference through a nonlinear medium [29].

This work was supported by National Natural Science Foundation of China (no. 11274203) and the Ministerio de Economía y Competitividad under project FIS2013-44174-P, Spain.

References

1. W. X. Lin, S. Q. Lin, and J. H. Huang, J. Opt. Soc. Am. B **20**, 479 (2003).
2. Y.-F. Chen, Appl. Phys. B **70**, 475 (2000).

3. Y. P. Huang, C. Y. Cho, Y. J. Huang, and Y.-F. Chen, Opt. Express **20**, 5644 (2012).
4. Y. F. Lü, P. Zhai, J. Xia, X. H. Fu, and S. T. Li, J. Opt. Soc. Am. B **29**, 2352 (2012).
5. H. Y. Shen, T. Q. Lian, R. R. Zeng, Y. P. Zhou, and G. F. Yu, IEEE J. Quantum Electron. **25**, 144 (1989).
6. H. Zhu, C. Huang, G. Zhang, Y. Wei, L. Huang, J. Chen, W. Chen, and Z. Chen, Opt. Commun. **270**, 296 (2007).
7. Y. F. Lü, J. Xia, J. Zhang, X. H. Fu, and H. L. Liu, Appl. Opt. **53**, 5141 (2014).
8. G. A. Massey, Appl. Phys. Lett. **17**, 213 (1970).
9. C. Grivas, Prog. Quantum Electron. **35**, 159 (2011).
10. A. Kaminskii, *Laser Crystals: Their Physics and Properties* (Springer, 1990).
11. V. Petrov and F. Rotermund, Opt. Lett. **38**, 5090 (2013).
12. J. I. Mackenzie, IEEE J. Sel. Top. Quantum Electron. **13**, 626 (2007).
13. M. Pollnau, C. Grivas, L. Laversenne, J. S. Wilkinson, R. W. Eason, and D. P. Shepherd, Laser Phys. Lett. **4**, 560 (2007).
14. E. Cantelar, D. Jaque, and G. Lifante, Opt. Mater. **34**, 555 (2012).
15. K. M. Davis, K. Miura, N. Sugimoto, and K. Hirao, Opt. Lett. **21**, 1729 (1996).
16. G. Salamu, F. Jipa, M. Zamfirescu, and N. Pavel, Opt. Express **22**, 5177 (2014).
17. T. Calmano and S. Müller, IEEE J. Sel. Top. Quant. Electron. **21**, 1602213 (2015).
18. Q. Liu, S. Gross, P. Dekker, M. J. Withford, and M. J. Steel, Opt. Express **22**, 28037 (2014).
19. W. F. Silva, C. Jacinto, A. Benayas, J. R. Vázquez de Aldana, G. A. Torchia, F. Chen, Y. Tan, and D. Jaque, Opt. Lett. **35**, 916 (2010).
20. R. R. Gattass and E. Mazur, Nat. Photonics **2**, 219 (2008).
21. K. Sugioka and Y. Cheng, Light Sci. Appl. **3**, e149 (2014).
22. M. Ams, G. D. Marshall, P. Dekker, J. A. Piper, and M. J. Withford, Laser Photon. Rev. **3**, 535 (2009).
23. C. Grivas, C. Corbari, G. Brambilla, G. Pavlos, and P. G. Lagoudakis, Opt. Lett. **37**, 4630 (2012).
24. F. Chen and J. R. Vázquez de Aldana, Laser Photon. Rev. **8**, 251 (2014).
25. A. G. Okhrimchuk, A. V. Shestakov, I. Khrushchev, and J. Mitchell, Opt. Lett. **30**, 2248 (2005).
26. N. Pavel, G. Salamu, F. Jipa, and M. Zamfirescu, Opt. Express **22**, 23057 (2014).
27. Y. Y. Ren, J. R. Vázquez de Aldana, F. Chen, and H. J. Zhang, Opt. Express **21**, 6503 (2013).
28. S. J. Field, D. C. Hanna, D. P. Shepherd, A. C. Tropper, P. J. Chandler, P. D. Townsend, and L. Zhang, Electron. Lett. **26**, 1826 (1990).
29. H. H. Yu, H. J. Zhang, Z. P. Wang, J. Y. Wang, Y. G. Yu, X. Y. Zhang, R. J. Lan, and M. H. Jiang, Appl. Phys. Lett. **94**, 041126 (2009).